Research Article Vol. 8, No. 4 / April 2021 / Optica 545

optica

All-optical single-shot complete electric field measurement of extreme ultraviolet free electron laser pulses

William K. Peters,[1] Travis Jones,[1,2] Anatoly Efimov,[1] Emanuele Pedersoli,[3] Laura Foglia,[3] Riccardo Mincigrucci,[3] Ivaylo Nikolov,[3] Rick Trebino,[2] Miltcho B. Danailov,[3] Flavio Capotondi,[3] Filippo Bencivenga,[3] and Pamela Bowlan[1,*]

[1]Los Alamos National Lab, Los Alamos, New Mexico 87544, USA
[2]School of Physics, Georgia Institute of Technology, Atlanta, Georgia 30332, USA
[3]Elettra-Sincrotrone Trieste S.C.p.A., S.S. 14 km 163,5 in Area Science Park, Basovizza, 34149 Trieste, Italy
*Corresponding author: pambowlan@lanl.gov

Received 1 December 2020; revised 24 February 2021; accepted 28 February 2021 (Doc. ID 416463); published 12 April 2021

Recent advances in ultrafast extreme ultraviolet (EUV) and x-ray light sources provide direct access to fundamental time and length scales for biology, chemistry, and materials physics. However, such light pulses are challenging to measure due to the need for femtosecond time resolution at difficult-to-detect wavelengths. Also, single-shot measurements are needed because severe pulse-to-pulse fluctuations are common. Here we demonstrate single-shot, complete field measurements by applying a novel version of frequency resolved optical gating. An EUV free electron laser beam creates a transient grating containing the pulse's electric field information, which is read out with a 400 nm probe pulse. By varying the time delay between two copies of the EUV pump, rather than between the pump and the probe, we separate the needed coherent wave mixing from the slow incoherent response. Because this approach uses photoionization, it should be applicable from the vacuum ultraviolet to hard x rays.

https://doi.org/10.1364/OPTICA.416463

1. INTRODUCTION

Ultrafast extreme ultraviolet (EUV) and x-ray free electron lasers (FELs) promise truly new insights by combining the coherence of lasers with x-ray scattering and spectroscopy [1–3]. However, to fully realize this potential, new diagnostics for complete field (amplitude and phase) measurement of these pulses are needed [4–7]. Most FELs display significant jitter in intensity, spectrum, and pulse duration, which limits signal-to-noise ratio and resolution. Shot-by-shot measurements of the pulse shapes would ameliorate many of these limitations. Also, more complete diagnostics can lead to better understanding and control, including new capabilities to produce subfemtosecond pulses [8] and two-color pulses [9]. Moreover, complete field measurements would extend broadband phase-sensitive spectroscopies like 2D spectroscopy to shorter wavelengths [10].

Femtosecond pulses cannot be fully characterized with typical electronics, which are far too slow. However, attosecond resolution is accessible with nonlinear optics, where the light–matter interaction provides a fast "shutter." This concept is widely used, for example, in frequency resolved optical gating (FROG) [11], which allows the electric field to be extracted from a spectrally resolved nonlinear optical signal versus delay (the FROG trace). A wide variety of nonlinear processes may be employed for FROG, although an instantaneous material response is preferred.

Extending FROG to shorter wavelengths is problematic for several reasons: first, short-wavelength spectrometers are low throughput; second, nonlinear optics with EUV and x-ray pulses is in its infancy, with few reports [12–14] demonstrating coherent wave mixing; and third, the dominant process is photoionization, with a slow material recovery. These difficulties have led to the use of photoelectron-based techniques for measuring EUV and x-ray pulses [6,7,15–19]. While photoelectron techniques have many advantages, extending the suite of optical FROG techniques to higher frequencies could allow for new capabilities such as single-shot and spatiotemporal characterization of FEL pulses.

In this paper we demonstrate an optically detected measurement of short-wavelength femtosecond pulses, addressing each challenge. First, diffracting an optical probe from an EUV-induced grating transfers the EUV pulse information to an optical field and allows detection with a standard visible camera and a single-shot geometry. Transient gratings have long been used for FROG [11], but the potential of a transient grating cross-correlation FROG (XFROG) to shift detection to a convenient wavelength was only recently recognized [20]. Second, introducing pulse-front tilt in the probe beam allows for sufficient time resolution [21] despite severe phase-matching angles, making it possible to identify

the short-lived coherent four-wave-mixing (FWM) response of interest. Third, scanning the EUV pulse-pair separation uses the dephasing time of photoionization as a fast time-gate [22]. We present a first demonstration of this concept by measuring the intensity and phase of 31.3 nm pulses at the FERMI FEL [2].

2. METHOD

Figure 1 summarizes our experimental concept. Two copies of the EUV beam [Fig. 1(a)] create an interference pattern, causing a spatial modulation in the sample's optical properties known as a transient grating [23]. An optical probe diffracts from the perturbed sample, gaining information about the material response and the EUV pulses. For optimal efficiency, the probe incidence angle should satisfy the phase matching, or Bragg, condition [23]; the large wavelength difference requires a steep probe angle (∼45°). Unfortunately, steep angles would decrease time resolution to more than a picosecond because the probe averages over a time range $\delta t = (w/c)\tan\theta_{\mathrm{opt}}$, where w is the probe beam width and c is the speed of light. Since the coherent FWM here is very short-lived, this averaging would likely blur the needed information. We overcome this by using a grism (a convenient combination of a grating and prism to avoid angular deviation) to introduce pulse-front tilt, so that the optical pulse front impinges parallel to the sample surface [24,25]. Imaging the grism onto the sample avoids any spatial chirp or pulse-front tilt [21]. Figure 1(b) also shows how the crossing angle is used to map EUV pulse-pair delay to position for single-shot measurements. Imaging the sample along the in-page direction and spectrally resolving along the out-of-page direction yields the FROG trace. A novel phase retrieval algorithm, taking the material response into account, is applied to extract the amplitude and phase of single EUV pulses from the FROG traces [Fig. 1(c)].

To demonstrate this method, experiments were carried out at the DiProI end-station equipped with the mini-TIMER split and delay line [26] at FERMI [2]. The FEL was operated at 50 Hz, with a bunch charge of about 600 pC and bunch length over 1 ps. The EUV pulses were centered at 31.1 nm and obtained by tuning the FEL to the eighth harmonic of a 249 nm seed laser. The EUV pulse was split into a pair of beams using the hard edge of a mirror before being crossed and focused on the sample, which was a free-standing 500 nm Si_3N_4 film. The energy and spot size of the EUV pump pulses at the Si_3N_4 sample were ∼30 μJ total in a 100 μm × 800 μm line focus, or a fluence of ∼38 mJ/cm^2. For generating test FEL pulses, the FEL seed pulse was chirped by about 2290 fs^2 by inserting 10 mm UV fused silica in the seed pulse. For generating structured low-temporal-coherence test pulses, the transversal coherence of the FEL pulse was controlled by means of the magnetic strength of the R56 dispersive section [7,27]. The spectrum of each EUV pulse was recorded upstream of the experiment with a grating spectrometer [28].

The optical probe was generated from an 8 μJ, 785 nm pulse from the same laser used to seed the FERMI FEL and had an RMS timing jitter with respect to the FEL pulses of about 6–7 fs [29] and a 50 fs pulse duration. This pulse was frequency doubled in a 0.4 mm beta-barium borate (BBO) crystal and narrowed with a bandpass filter (Edmund Optics model 12-276) to obtain a 150 nJ, 104 fs pulse at 397 nm, which was incident on the sample at approximately 45°. The grism was a 1870 line/mm transmission grating between two 42° apex UV fused silica prisms (Wasatch Photonics) and was imaged onto the sample in the horizontal direction with a pair of cylindrical lenses. The grism was inserted a minimum amount into the beam in order to minimize temporal dispersion (∼1000 fs^2). A separate cylindrical lens was used to focus in the vertical direction and produce a spot size matching the FEL beams. During data collection, the probe remained at a constant time delay, typically between −200 and 0 fs. The diffracted probe (the nonlinear signal) was imaged onto the detection camera (PI-MTE2048, 13.5 μm pixel size) with a pair of 50 mm spherical lenses, between which a 1000 gr/mm grism (also from Wasach Photonics) was placed. This grism was oriented to disperse along the vertical dimension so that wavelength was mapped to the vertical direction.

The pump beams were incident at 3.35° to either side of the surface normal. Phase matching, which here can be expressed as $\sin\theta_{\mathrm{opt}} = (\lambda_{\mathrm{opt}}/\lambda_{\mathrm{euv}})\sin\theta_{\mathrm{euv}}$, required the pulse be incident at 49°. Because the pump absorption length in our silicon nitride sample is very short (25 nm), this phase-matching condition is not strict, and a 45° incidence angle for the probe gave acceptable signal. The EUV crossing angle and spot size provided a pump-pair time range of 300 fs, while the sample-to-detector imaging conditions and camera pixel size give a time step of 5.49 fs. The time resolution of a FROG electric field retrieval depends on this step size and the spectral bandwidth of the detected signal. As a single-shot technique, the resolution is unaffected by timing jitter.

3. RESULTS AND DISCUSSION

The two transient grating measurements in Fig. 2 illustrate how the FEL pulse amplitude and phase can be measured using photoionization as the material response. In Fig. 2(b), the optical probe pulse delay was scanned (i.e., a pump-probe measurement), and in Fig. 2(c) the delay between the two FEL pulses, or the pump-pump delay, was scanned. FROG almost always uses an instantaneous nonlinear response (with notable exceptions [30,31]); but here the light–matter interaction is dominated by photoionization [Fig. 2(a)] and has a long recovery time of hundreds of picoseconds or more as shown in the probe scan in Fig. 2(b) [32]. Consequently, extracting the FEL pulse from the probe scan would require a challenging deconvolution [7,33,34]. Instead, we can use the transient grating to separate the coherent FWM interaction, present only near time zero, from the long-lived part of the signal, by instead scanning the pump-pump delay. This works because a grating is only created if the material polarization induced by the first copy of the pump survives until the second copy arrives; this time scale is the dephasing time, and it is related to the free induction decay [22]. By choosing a sample with a featureless absorption spectrum at the pump wavelength, the dephasing time will be nearly instantaneous. Consequently, even though the pump-excited sample has a slow recovery, the transient grating signal as a function of pump-pump delay roughly resembles a cross-correlation made using an instantaneous medium as seen in Fig. 2(c) [35].

The data in Fig. 2 also show that the FWM signal during pulse overlap contains the bandwidth of the EUV pulse. Physically, an ionized atom supports a material polarization until the outgoing wavepacket loses spatial overlap with its hole. After that, the nonlinear signal contains only frequencies already in the probe, has no phase relationship with the pump, and can be considered an incoherent pump-probe signal. The difference between coherent FWM and incoherent pump-probe signal is demonstrated in Fig. 2(b) by the increase in bandwidth at time zero compared to

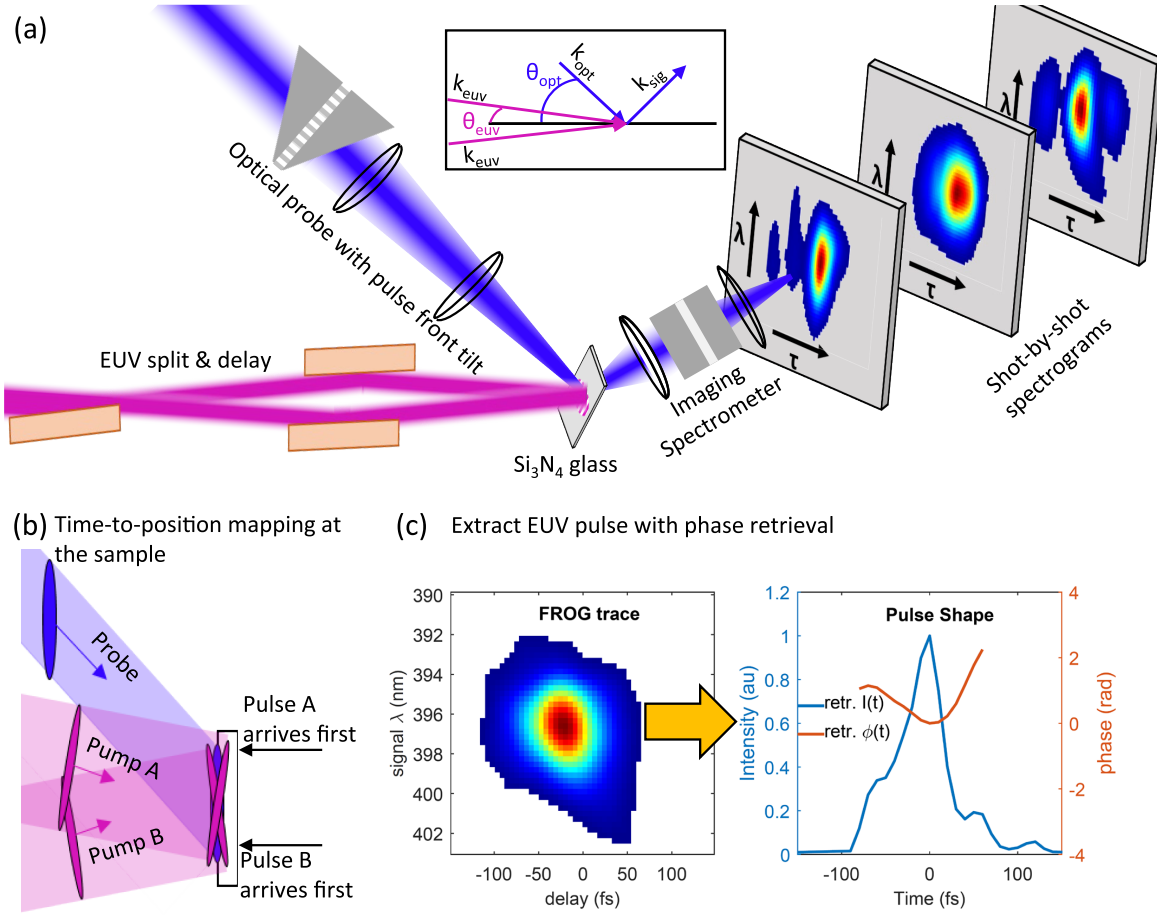

Fig. 1. Encoding the pulse shape of a single EUV pulse in an optical nonlinear signal. (a) EUV pulse information is transferred to a visible probe pulse. (b) A line focus allows for single-shot measurement, where the crossing angle between two to pump beams maps their delay with respect to one another into position. (c) The complete electric field is extracted from each FROG trace. The diagram in (a) is a view from above at a slight angle and that in (b) is a view from above.

later times. By inspection of Figs. 2(b) and 2(c), we see that this extra bandwidth is present in Fig. 2(c), suggesting that the coherent FWM response is preserved in the pump-delay scans.

Therefore, we can implement FROG in the EUV using photoionization and scanning the pump-pump delay as done in Fig. 2(c). While this largely isolates the coherent FWM, there remains some incoherent response that must be taken into account. The FROG trace is

$$I_{\mathrm{FROG}}(\omega, \tau) = |\mathcal{F}(E_{\mathrm{sig}}(t, \tau))|^2,$$

where $\mathcal{F}(t)$ indicates a Fourier transformation. We use an empirical model for the signal field:

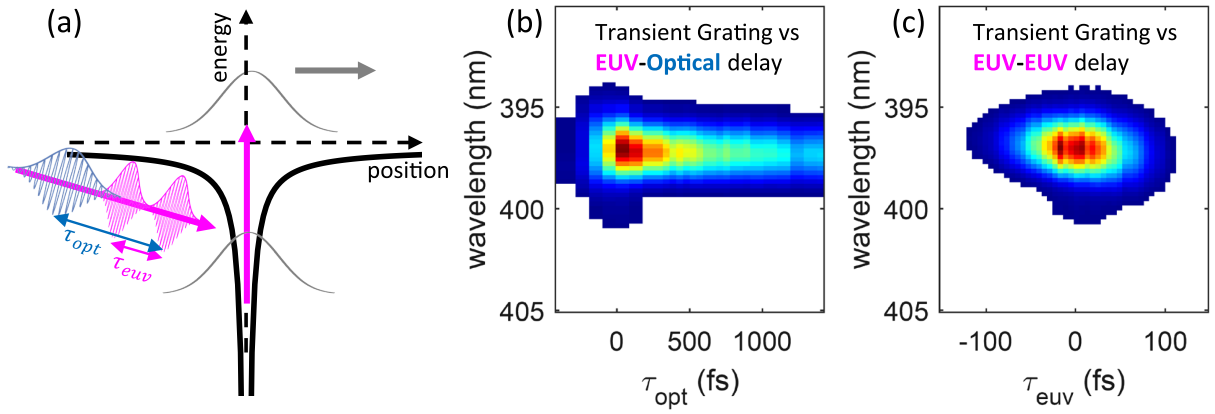

Fig. 2. Isolating the coherent material response. (a) An electron absorbs a single photon from the EUV pulse pair. While the outgoing wavepacket overlaps the nascent hole, a coherent polarization exists. (b) The spectrally resolved signal versus pump-probe delay reveals coherent wave mixing during pulse overlap and a long-lived incoherent response. (c) Signal versus pump-pair separation provides a quasi-instantaneous response, preserving the coherent wave mixing.

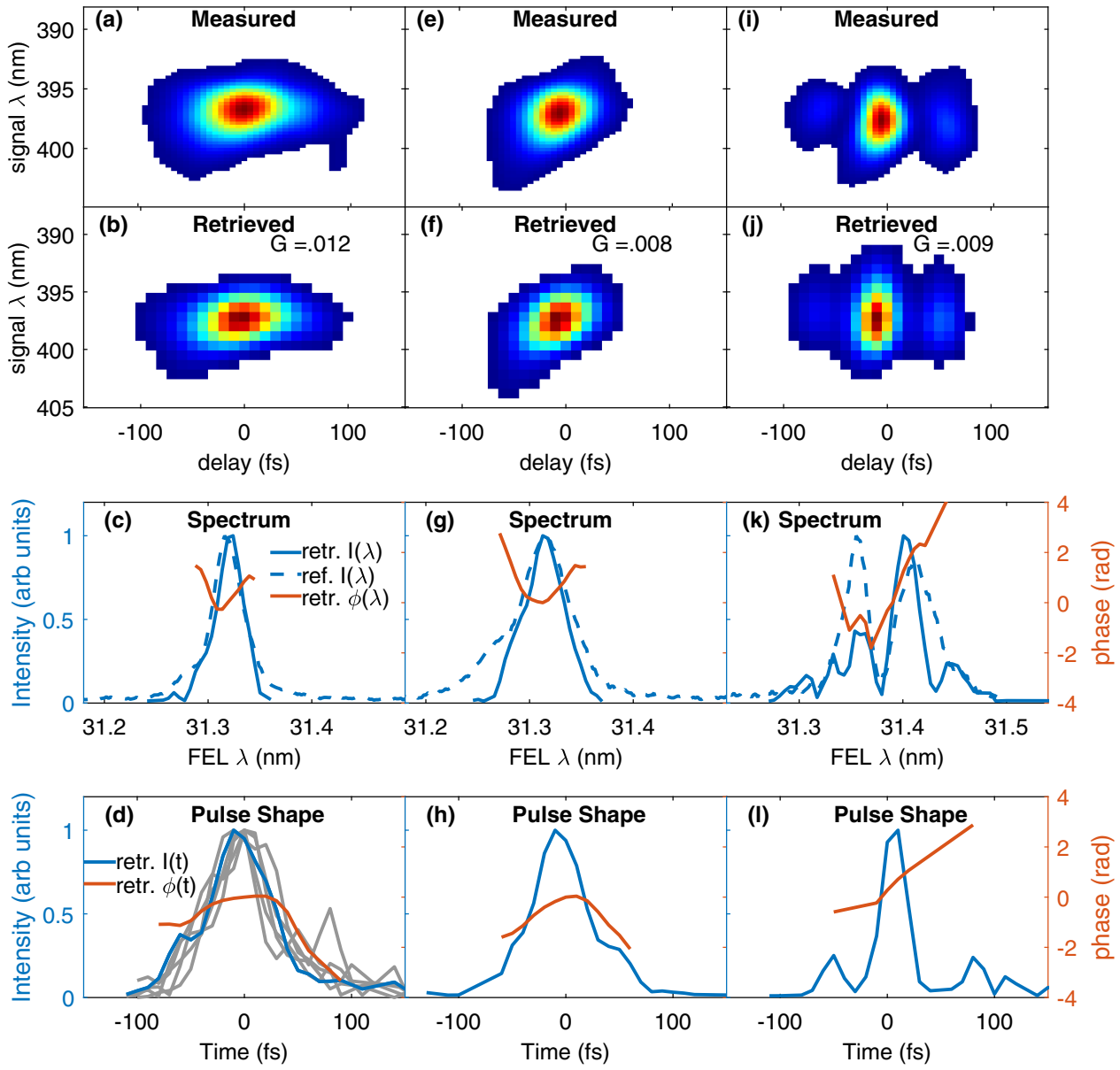

Fig. 3. Measurements of single EUV pulses: Top row, left to right: measured traces under standard conditions, with a chirped seed laser, and with low temporal coherence. Second row: reconstructed traces. Third row: retrieved spectral fields and independently measured spectra. Bottom row: retrieved temporal fields.

$$E_{\mathrm{sig}}(t,\tau_{\mathrm{euv}}) = E_{\mathrm{opt}}(t-\tau_{\mathrm{opt}})\int_{-\infty}^{t} R(t-t')E_{\mathrm{euv}}(t')E^{*}_{\mathrm{euv}}(t'-\tau_{\mathrm{euv}})\mathrm{d}t'.$$

$R(t)$ is the material response function given by

$$R(t) = \delta(t) + c_\theta \Theta(t),$$

where $\delta(t)$ is the Dirac delta function representing the coherent FWM, $\Theta(t)$ is the Heaviside step function representing the incoherent part of the response, and c_θ is an adjustable complex constant (see Supplement 1). This model describes an instantaneous dephasing and assumes the ground-state recovery is slow compared to the pulses. We find this simple model sufficient for applying phase retrieval to extract the EUV field.

Figure 3 shows measured single-shot FROG traces along with the results of phase retrieval. The left-side column shows a measurement under FERMI's standard conditions and represents a typical pulse. The measured spectrogram reveals a small amount of chirp in the tilt, and the overall shape appears well represented in the retrieved trace. Figure 3(c) shows the retrieved spectral intensity and phase compared to an independently measured spectrum of the same pulse, showing a good match except for the tails. Figure 3(d) shows the retrieved pulse as a function of time, which shows a main pulse that is reasonably fit by a 71 ± 6 fs Gaussian, compared to the predicted 70 fs [7]. Gray lines are retrieved intensities for several other pulses, showing good pulse-to-pulse stability as expected from a seeded FEL.

As a seeded FEL, FERMI uses an optical "seed" laser to manipulate its electron bunch in order to control the emission of EUV light. There is much interest in shaping the seed pulse to achieve

more sophisticated control over the EUV pulse. The middle column of Fig. 3, therefore, shows a measurement while chirping the seed laser, which produced more bandwidth. Interestingly, although the trace appears significantly narrowed in time, the retrieved electric field is only modestly shorter (60 fs) than in the standard configuration. This comes from the residual incoherent signal, which dominates the central portion of the spectrogram and is not indicative of pulse shape. The right-side column shows a measurement made with a low-temporal-coherence FEL beam, which produced structured pulses. For these two columns, despite low retrieval errors, there are discrepancies remaining in the retrieved spectra compared to the reference spectra. This likely stems primarily from signal-to-noise limitations in these measurements, making it more difficult to measure weaker features or the tails of the FROG traces. Our signal-to-noise ratio was limited by probe scatter inside the EUV vacuum chamber, which could be straightforwardly improved in future work. The accuracy of the model could also introduce some error, but from our simulations (see Supplement 1), this is expected to play a minor role.

The EUV electric fields were extracted from the FROG traces using a General Projections algorithm. We used derivative-free downhill simplex minimization routine to implement the projection to the mathematical form constraint set. The projection to the data constraint set is implemented by spectrogram magnitude replacement as is typical. Single-shot spectrograms were Fourier filtered to remove noise, real-space filtered to remove residual probe scatter, and binned into a 64×64 grid with 10 fs steps prior to running the phase retrieval algorithm. The retrievals shown in Fig. 3 used $c_\theta = 0.67\exp(i\pi/4)$ and required 50 iterations, which took about 6 min; however, straightforward improvements in the algorithm, such as using a gradient-based optimization and a faster programing language, should make this significantly faster. Retrieval quality is judged with the "G" error [11], $G = \mathrm{sqrt}\left(\sum_{i,j}^{N} |I_{\mathrm{meas}}(\omega_i, \tau_j) - \mu I_{\mathrm{ret}}(\omega_i, \tau_j)|^2 / N^2\right)$, with ~1% being considered the threshold for a good retrieval. See Supplement 1 for more details on the phase retrieval algorithm.

4. CONCLUSION

In summary, we report a novel, all-optical measurement of the pulse shape of short-wavelength FEL pulses that we believe will be generally useful across the EUV, soft- and hard-x-ray spectral ranges, and also to tabletop EUV sources. Single-shot measurements were achieved, paving the way for online diagnostics of detailed pulse shapes at x-ray FEL facilities.

Funding. U.S. Department of Energy (LANL African American Partnership Program, LANL-LDRD-ER20180242).

Disclosures. RT: Swamp Optics (I).

Data Availability. Data underlying the results presented in this paper are not publicly available at this time but may be obtained from the authors upon reasonable request.

Supplemental document. See Supplement 1 for supporting content.

REFERENCES

1. W. Helml, I. Grguraš, P. Juranić, S. Düsterer, T. Mazza, A. R. Maier, N. Hartmann, M. Ilchen, G. Hartmann, L. Patthey, C. Callegari, J. T. Costello, M. Meyer, R. N. Coffee, A. L. Cavalieri, and R. Kienberger, "Ultrashort free-electron laser x-ray pulses," Appl. Sci. **7**, 915–955 (2017).
2. E. Allaria, R. Appio, L. Badano, W. A. Barletta, S. Bassanese, S. G. Biedron, A. Borga, E. Busetto, D. Castronovo, P. Cinquegrana, S. Cleva, D. Cocco, M. Cornacchia, P. Craievich, I. Cudin, G. D'Auria, M. Dal Forno, M. B. Danailov, R. De Monte, G. De Ninno, P. Delgiusto, A. Demidovich, S. Di Mitri, B. Diviacco, A. Fabris, R. Fabris, W. Fawley, M. Ferianis, E. Ferrari, S. Ferry, L. Froehlich, P. Furlan, G. Gaio, F. Gelmetti, L. Giannessi, M. Giannini, R. Gobessi, R. Ivanov, E. Karantzoulis, M. Lonza, A. Lutman, B. Mahieu, M. Milloch, S. V. Milton, M. Musardo, I. Nikolov, S. Noe, F. Parmigiani, G. Penco, M. Petronio, L. Pivetta, M. Predonzani, F. Rossi, L. Rumiz, A. Salom, C. Scafuri, C. Serpico, P. Sigalotti, S. Spampinati, C. Spezzani, M. Svandrlik, C. Svetina, S. Tazzari, M. Trovo, R. Umer, A. Vascotto, M. Veronese, R. Visintini, M. Zaccaria, D. Zangrando, and M. Zangrando, "Highly coherent and stable pulses from the FERMI seeded free-electron laser in the extreme ultraviolet," Nat. Photonics **6**, 699–704 (2012).
3. C. Bostedt, S. Boutet, D. M. Fritz, Z. Huang, H. J. Lee, H. T. Lemke, A. Robert, W. F. Schlotter, J. J. Turner, and G. J. Williams, "Linac coherent light source: the first five years," Rev. Mod. Phys. **88**, 015007 (2016).
4. S. Düsterer, M. Rehders, A. Al-Shemmary, C. Behrens, G. Brenner, O. Brovko, M. DellAngela, M. Drescher, B. Faatz, J. Feldhaus, U. Frühling, N. Gerasimova, N. Gerken, C. Gerth, T. Golz, A. Grebentsov, E. Hass, K. Honkavaara, V. Kocharian, M. Kurka, Th. Limberg, R. Mitzner, R. Moshammer, E. Plönjes, M. Richter, J. Rönsch-Schulenburg, A. Rudenko, H. Schlarb, B. Schmidt, A. Senftleben, E. A. Schneidmiller, B. Siemer, F. Sorgenfrei, A. Sorokin, N. Stojanovic, K. Tiedtke, R. Treusch, M. Vogt, M. Wieland, W. Wurth, S. Wesch, M. Yan, M. V. Yurkov, H. Zacharias, and S. Schreiber, "Development of experimental techniques for the characterization of ultrashort photon pulses of extreme ultraviolet free-electron lasers," Phys. Rev. ST Accel. Beams **17**, 120702 (2014).
5. R. N. Coffee, J. P. Cryan, J. Duris, W. Helml, S. Li, and A. Marinelli, "Development of ultrafast capabilities for x-ray free-electron lasers at the Linac Coherent Light Source," Philos. Trans. A **377**, 20180386 (2019).
6. N. Hartmann, G. Hartmann, R. Heider, M. S. Wagner, M. Ilchen, J. Buck, A. O. Lindahl, C. Benko, J. Grünert, J. Krzywinski, J. Liu, A. A. Lutman, A. Marinelli, T. Maxwell, A. A. Miahnahri, S. P. Moeller, M. Planas, J. Robinson, A. K. Kazansky, N. M. Kabachnik, J. Viefhaus, T. Feurer, R. Kienberger, R. N. Coffee, and W. Helml, "Attosecond time–energy structure of x-ray free-electron laser pulses," Nat. Photonics **12**, 215–220 (2018).
7. P. Finetti, H. Höppner, E. Allaria, C. Callegari, F. Capotondi, P. Cinquegrana, M. Coreno, R. Cucini, M. B. Danailov, A. Demidovich, G. De Ninno, M. Di Fraia, R. Feifel, E. Ferrari, L. Fröhlich, D. Gauthier, T. Golz, C. Grazioli, Y. Kai, G. Kurdi, N. Mahne, M. Manfredda, N. Medvedev, I. P. Nikolov, E. Pedersoli, G. Penco, O. Plekan, M. J. Prandolini, K. C. Prince, L. Raimondi, P. Rebernik, R. Riedel, E. Roussel, P. Sigalotti, R. Squibb, N. Stojanovic, S. Stranges, C. Svetina, T. Tanikawa, U. Teubner, V. Tkachenko, S. Toleikis, M. Zangrando, B. Ziaja, F. Tavella, and L. Giannessi, "Pulse duration of seeded free-electron lasers," Phys. Rev. X **7**, 021043 (2017).
8. A. A. Zholents and W. M. Fawley, "Proposal for intense attosecond radiation from an x-ray free-electron laser," Phys. Rev. Lett. **92**, 224801 (2004).
9. A. A. Lutman, T. J. Maxwell, J. P. MacArthur, M. W. Guetg, N. Berrah, R. N. Coffee, Y. Ding, Z. Huang, A. Marinelli, S. Moeller, and J. C. U. Zemella, "Fresh-slice multicolour x-ray free-electron lasers," Nat. Photonics **10**, 745–750 (2016).
10. M. Kowalewski, B. P. Fingerhut, K. E. Dorfman, K. Bennett, and S. Mukamel, "Simulating coherent multidimensional spectroscopy of nonadiabatic molecular processes: from the infrared to the x-ray regime," Chem. Rev. **117**, 12165–12226 (2017).
11. R. Trebino, *Frequency-Resolved Optical Gating: The Measurement of Ultrashort Laser Pulses* (Kluwer Academic Publishers, 2002).
12. C. Svetina, R. Mankowsky, G. Knopp, F. Koch, G. Seniutinas, B. Rösner, A. Kubec, M. Lebugle, I. Mochi, M. Beck, C. Cirelli, J. Krempasky, C. Pradervand, J. Rouxel, G. F. Mancini, S. Zerdane, B. Pedrini, V. Esposito, G. Ingold, U. Wagner, U. Flechsig, R. Follath, M. Chergui, C. Milne, H. T. Lemke, C. David, and P. Beaud, "Towards x-ray transient grating spectroscopy," Opt. Lett. **44**, 574–577 (2019).
13. T. E. Glover, D. M. Fritz, M. Cammarata, T. K. Allison, S. Coh, J. M. Feldkamp, H. Lemke, D. Zhu, Y. Feng, R. N. Coffee, M. Fuchs, S. Ghimire, J. Chen, S. Shwartz, D. A. Reis, S. E. Harris, and J. B. Hastings, "X-ray and optical wave mixing," Nature **488**, 603–608 (2012).

14. F. Bencivenga, F. Capotondi, R. Mincigrucci, R. Cucini, M. Manfredda, E. Pedersoli, E. Principi, A. Simoncig, and C. Masciovecchio, "Nonlinear optics with coherent free electron lasers," Phys. Scr. **T169**, 014003 (2016).
15. Y. Mairesse and F. Quéré, "Frequency-resolved optical gating for complete reconstruction of attosecond bursts," Phys. Rev. A **71**, 011401 (2005).
16. I. Grguraš, A. R. Maier, C. Behrens, T. Mazza, T. J. Kelly, P. Radcliffe, S. Düsterer, A. K. Kazansky, N. M. Kabachnik, Th. Tschentscher, J. T. Costello, M. Meyer, M. C. Hoffmann, H. Schlarb, and A. L. Cavalieri, "Ultrafast x-ray pulse characterization at free-electron lasers," Nat. Photonics **6**, 852–857 (2012).
17. U. Frühling, M. Wieland, M. Gensch, T. Gebert, B. Schütte, M. Krikunova, R. Kalms, F. Budzyn, O. Grimm, J. Rossbach, E. Plönjes, and M. Drescher, "Single-shot terahertz-field-driven x-ray streak camera," Nat. Photonics **3**, 523–528 (2009).
18. R. Mitzner, A. A. Sorokin, B. Siemer, S. Roling, M. Rutkowski, H. Zacharias, M. Neeb, T. Noll, F. Siewert, W. Eberhardt, M. Richter, P. Juranic, K. Tiedtke, and J. Feldhaus, "Direct autocorrelation of soft-x-ray free-electron-laser pulses by time-resolved two-photon double ionization of He," Phys. Rev. A **80**, 025402 (2009).
19. A. Azima, J. Bödewadt, O. Becker, S. Düsterer, N. Ekanayake, R. Ivanov, M. M. Kazemi, L. L. Lazzarino, C. Lechner, T. Maltezopoulos, B. Manschwetus, V. Miltchev, J. Müller, T. Plath, A. Przystawik, M. Wieland, R. Assmann, I. Hartl, T. Laarmann, J. Rossbach, W. Wurth, and M. Drescher, "Direct measurement of the pulse duration and frequency chirp of seeded XUV free electron laser pulses," New J. Phys. **20**, 013010 (2018).
20. T. Jones, W. K. Peters, A. Efimov, R. L. Sandberg, D. Yarotski, R. Trebino, and P. Bowlan, "Encoding the complete electric field of an ultraviolet ultrashort laser pulse in a near-infrared nonlinear-optical signal," Opt. Express **28**, 26850–26860 (2020).
21. A. A. Maznev, T. F. Crimmins, and K. A. Nelson, "How to make femtosecond pulses overlap," Opt. Lett. **23**, 1378–1380 (1998).
22. A. M. Weiner, *Ultrafast Optics* (Wiley & Sons, 2009).
23. H. J. Eichler, P. Günter, and D. W. Pohl, *Laser-Induced Dynamic Gratings* (Springer, 1986).
24. Z. Bor, B. Racz, G. Szabo, M. Hilbert, and H. A. Hazim, "Femtosecond pulse front tilt caused by angular dispersion," Opt. Eng. **32**, 2501–2505 (1993).
25. S. Akturk, X. Gu, P. Gabolde, and R. Trebino, "The general theory of first-order spatio-temporal distortions of Gaussian pulses and beams," Opt. Express **13**, 8642–8661 (2005).
26. R. Mincigrucci, L. Foglia, D. Naumenko, E. Pedersoli, A. Simoncig, R. Cucini, A. Gessini, M. Kiskinova, G. Kurdi, N. Mahne, M. Manfredda, I. P. Nikolov, E. Principi, L. Raimondi, M. Zangrando, C. Masciovecchio, F. Capotondi, and F. Bencivenga, "Advances in instrumentation for FEL-based four-wave-mixing experiments," Nucl. Instrum. Meth. A **907**, 132–148 (2018).
27. L. Foglia, F. Capotondi, H. Höppner, A. Gessini, L. Giannessi, G. Kurdi, I. Lopez Quintas, C. Masciovecchio, M. Kiskinova, R. Mincigrucci, D. Naumenko, I. P. Nikolov, E. Pedersoli, G. M. Rossi, A. Simoncig, and F. Bencivenga, "Exploring the multiparameter nature of EUV-visible wave mixing at the FERMI FEL," Struct. Dyn. **6**, 040901 (2019).
28. C. Svetina, D. Cocco, N. Mahne, L. Raimondi, E. Ferrari, and M. Zangrando, "PRESTO, the on-line photon energy spectrometer at FERMI: design, features and commissioning results," J. Synchrotron Radiat. **23**, 35–42 (2016).
29. M. B. Danailov, F. Bencivenga, F. Capotondi, F. Casolari, P. Cinquegrana, A. Demidovich, E. Giangrisostomi, M. P. Kiskinova, G. Kurdi, M. Manfredda, C. Masciovecchio, R. Mincigrucci, I. P. Nikolov, E. Pedersoli, E. Principi, and P. Sigalotti, "Towards jitter-free pump-probe measurements at seeded free electron laser facilities," Opt. Express **22**, 12869–12879 (2014).
30. K. W. DeLong, C. L. Ladera, R. Trebino, B. Kohler, and K. R. Wilson, "Ultrashort-pulse measurement using noninstantaneous nonlinearities: Raman effects in frequency-resolved optical gating," Opt. Lett. **20**, 486–488 (1995).
31. A. Leblanc, P. Lassonde, S. Petit, J.-C. Delagnes, E. Haddad, G. Ernotte, M. R. Bionta, V. Gruson, B. E. Schmidt, H. Ibrahim, E. Cormier, and F. Légaré, "Phase-matching-free pulse retrieval based on transient absorption in solids," Opt. Express **27**, 28998–29015 (2019).
32. C. Gahl, A. Azima, M. Beye, M. Deppe, K. Döbrich, U. Hasslinger, F. Hennies, A. Melnikov, M. Nagasono, A. Pietzsch, M. Wolf, W. Wurth, and A. Föhlisch, "A femtosecond x-ray/optical cross-correlator," Nat. Photonics **2**, 165–169 (2008).
33. D. J. Kane, N. Hartmann, R. N. Coffee, and A. R. Fry, "Experimental and analysis considerations for transmission/reflection spectrograms used in ultrafast x-ray pulse diagnostics," Proc. SPIE **9740**, 97400H (2016).
34. R. Riedel, A. Al-Shemmary, M. Gensch, T. Golz, M. Harmand, N. Medvedev, M. J. Prandolini, K. Sokolowski-Tinten, S. Toleikis, U. Wegner, B. Ziaja, N. Stojanovic, and F. Tavella, "Single-shot pulse duration monitor for extreme ultraviolet and x-ray free-electron lasers," Nat. Commun. **4**, 1731 (2013).
35. F. Capotondi, L. Foglia, M. Kiskinova, C. Masciovecchio, R. Mincigrucci, D. Naumenko, E. Pedersoli, A. Simoncig, and F. Bencivenga, "Characterization of ultrafast free-electron laser pulses using extreme-ultraviolet transient gratings," J. Synchrotron Radiat. **25**, 32–38 (2018).